Effects of Chain Rigidity on the Adsorption of a Polyelectrolyte Chain on Mixed Lipid Monolayer: A Monte Carlo Study

ARTICLE *in* THE JOURNAL OF PHYSICAL CHEMISTRY B · APRIL 2015

Impact Factor: 3.3 · DOI: 10.1021/acs.jpcb.5b00515 · Source: PubMed

THE JOURNAL OF PHYSICAL CHEMISTRY B

Article

pubs.acs.org/JPCB

Effects of Chain Rigidity on the Adsorption of a Polyelectrolyte Chain on Mixed Lipid Monolayer: A Monte Carlo Study

Xiaozheng Duan,[†] Mingming Ding,[†] Ran Zhang,[†] Liangyi Li,[†] Tongfei Shi,*[,†] Lijia An,[†] Qingrong Huang,[‡] and Wen-Sheng Xu*[,§]

[†]State Key Laboratory of Polymer Physics and Chemistry, Changchun Institute of Applied Chemistry, Chinese Academy of Sciences, Changchun, 130022, P. R. China

[‡]Department of Food Science, Rutgers University, 65 Dudley Road, New Brunswick, New Jersey 08901, United States

[§]James Franck Institute, The University of Chicago, Chicago, Illinois 60637, United States

Supporting Information

ABSTRACT: We apply Monte Carlo simulation to explore the adsorption of a positively charged polyelectrolyte on a lipid monolayer membrane, composed of electronically neutral, monovalent anionic and mulvitalent anionic phospholipids. We systematically assess the influence of various factors, including the intrinsic rigidity of the polyelectrolyte chain, the bead charge density of the polyelectrolyte, and the ionic strength of the saline solution, on the interfacial structural properties of the polyelectrolyte/monolayer complex. The enhancement of the polyelectrolyte chain intrinsic rigidity reduces the polyelectrolyte conformational entropy loss and the energy gains in electrostatic interaction, but elevates the segregated anionic lipid demixing entropy loss. This energy-entropy competition results in a nonmonotonic dependence of the polyelectrolyte/monolayer association strength on the degree of chain rigidity. The semiflexible polyelectrolyte, i.e., the one with an intermediate degree of chain rigidity, is shown to associate onto the ternary membane below a higher critical ionic concentration. In this ionic concentration regime, the semiflexible polyelectrolyte binds onto the monolayer more firmly than the pancake-like flexible one and exhibits a stretched conformation. When the chain is very rigid, the polyelectrolyte with bead charge density Z_b = +1 exhibits a larger tail and tends to dissociate from the membrane, whereas the one with Z_b = +2 can still bind onto the membrane in a bridge-like conformation. Our results imply that chain intrinsic rigidity serves as an efficient molecular factor for tailoring the adsorption/desorption transition and interfacial structure of the polyelectrolyte/monolayer complex.

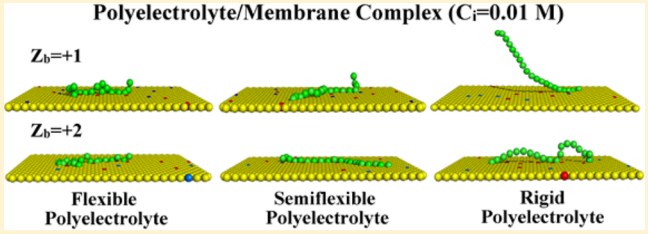

1. INTRODUCTION

The adsorption of cationic peripheral biomacromolecules onto the plasma membranes containing anionic lipid species is essential for a great number of cellular processes.[1−3] In the membrane, the dominant component for peripheral macromolecule association is the phosphatidylinositol 4,5-bisphosphate (PIP_2) lipids. This multivalent anionic signaling lipid species plays a key role in a variety of cellular functions,[1,2,4,5] although it comprises merely 1% of all phospholipids. Another important lipid species, the monovalent anionic phosphatidylserine (PS), comprises 10% to 20% of all phospholipids. PS lipids can significantly alter the membrane surface charge[6] and also play key roles in many biological activities.[3] The entropic gain from the counterion release of the charged macromolecule provides a considerable drive for the macromolecule adsorption on oppositely charged surfaces. Earlier experiments have illustrated that the energy gain from the electrostatic neutralization is the main force to associate the cationic macromolecule with the anionic lipids in the membranes, and that the hydrophobic interactions are negligible.[7−9] On the other hand, this electrostatic neutralization is opposed by the entropy loss induced by the macromolecule adsorption and the lipid demixing. These energetic and entropic effects compete to determine the structure and dynamics of the charged macromolecule/lipid complexes.

To comprehend the physical mechanisms in biological science and medical applications,[10−16] a large number of experimental studies have extensively investigated the properties of the charged macromolecule/lipid complexes.[8,17−21] Several studies have revealed that the adsorbing cationic macromolecules can cause the equilibrium[18,22−24] and dynamic heterogeneity[1,19,25] of the anionic lipids in membrane. Accordingly, the anionic lipids alter the properties of the peripheral macromolecules.[6,26] Because of the limitations in experiments on the phosphatidylinositol 4,5-bisphosphate (PIP_2) lipids due to their rapid hydrolysis,[1,16] over the past decades, a vast number of new theoretical and computational modeling methods have been established to better understand

Received: January 18, 2015
Revised: April 17, 2015
Published: April 23, 2015

DOI: 10.1021/acs.jpcb.5b00515
J. Phys. Chem. B 2015, 119, 6041−6049

the properties of the macromolecule/membrane complexes. For example, several novel coarse-grained models, where the macromolecules are coarse-grained in different shapes,[24,27−31] have been proposed to explore the mechanism of macromolecule adsorption and lipid segregation; the atomic-level models[5,32] have also been constructed to understand the balance between energy and entropy of the complexes.[5,7,33,34] In our previous work,[35−37] we have developed a Monte Carlo model to elucidate the properties of the complexes composed of a flexible cationic polyelectrolyte and an anionic membrane.

Previous studies have mainly focused on the effects of concentrations, sizes and charge amount of the macromolecules on the nature of macromolecule/membrane complexes, whereas, the stability of the complexes is known to be significantly influenced by another essential molecular factor, i.e., the flexibility of the adsorbing macromolecules. The peripheral proteins or polypeptides with different specific secondary structures or chemical compositions can display obvious distinctions in their intrinsic rigidities, resulting in drastic alterations in the equilibrium and dynamic properties of the macromolecule/lipid complexes[24,38] and the corresponding entropy-energy balances. Evidently, studies for the effects of macromolecule intrinsic rigidity on the structural variations of the complexes can lead to a better elucidating for the related mechanism of the association and offer the potential to develop therapeutic strategies through the controlled release of the signaling lipids.[2,4] Hence, the present paper extends the previous Monte Carlo simulation to explore the adsorption of a positively charged polyelectrolyte chain with tunable intrinsic rigidity on a lipid monolayer, composed of electronically neutral, monovalent anionic and mulvitalent anionic lipids.

In section 2, we briefly introduce our Monte Carlo model and the simulation details. In section 3, we discuss in detail how various factors, including the intrinsic rigidity of the polyelectrolyte chain, the bead charge density of the polyelectrolyte and the ionic concentration of the saline solution, cooperate to affect the adsorption/desorption transition of the complex, and further analyze how these factors alter the polyelectrolyte structural variation, the anionic lipid reorganization, the polyelectrolyte adsorption amount, and the monolayer surface coverage ratio. Our results are finally summarized in section 4.

2. SIMULATION METHOD

2.1. Model. The model employed in the present work is an extension of the model used in our previous work[35−38] and other studies for polyelectrolyte/membrane interactions.[24,31] Here, we briefly summarize the basic features of the model.

We adopt the simple flat hexagonal lattice plane to coarse-grain the lipid monolayer membrane, which locates at $z = 0$, with a total of 50 × 50 lattice grids representing the electrically neutral PC, monovalent anionic PS and tetravalent anionic PIP_2 lipid headgroups. The charge taken by each anionic lipid headgroup locates at the grid, and all lipid headgroups are coarse-grained as a hexagonal array of closely packed disks with the same diameter of d = 8.66 Å. In connection with the physiological focus, the present work investigates several monolayer compositions, including PC:PIP_2 = 99:1, PC:PS:PIP_2 = 98:1:1, PC:PS:PIP_2 = 89:10:1, and PC:PS=90:10. We employ the freely jointed chain model to coarse-grain the cationic polyelectrolyte,[39] which contains N = 20 connected physical beads. The diameter of a bead is d and each bead takes a charge at its center.

We describe the system potential energy as,

$$U = U_{\mathrm{Nbond}} + U_{\mathrm{Bond}} + U_{\mathrm{Angle}} \tag{1}$$

where U_{Bond} designates the contributions from the chain connectivity of the polyelectrolyte, and is set to be zero since the polyelectrolyte bond length is fixed as d in our model. The nonbonding energy (U_{Nbond}) is the sum of a hard sphere potential ($U_{\mathrm{H-S}}$) and a Coulomb potential (U_{Coul}),

$$U_{\mathrm{Nbond}} = U_{\mathrm{H-S}} + U_{\mathrm{Coul}} \tag{2}$$

The hard sphere potential ($U_{\mathrm{H-S}}$) ensures the excluded volume of the polyelectrolyte beads and the impenetrability of the monolayer. The Coulomb potential (U_{Coul}) accounts for the electrostatic interaction between charged species, i.e. polyelectrolyte beads and anionic lipids, via the Debye−Hückel approximation,

$$u_{\mathrm{el}}(r_{ij}) = Z_i Z_j l_{\mathrm{B}} \frac{\exp(-\kappa r_{ij})}{r_{ij}} \tag{3}$$

where r represents the distance between any two charged particles, Z denotes the charge at the center of each particle, and l_{B} is the Bjerrum length, which equals 7.14 Å at room temperature.

The polyelectrolyte/monolayer complex is in a monovalent salt solution with the ionic concentration of C_i. We account for the salt effects of the solution via κ (the Debye screening length), calculated from the ionic concentration C_i,

$$\kappa^2 = 1000 e^2 N_{\mathrm{A}} \sum_i \frac{Z_i^2 C_i}{\varepsilon_0 \varepsilon_r k_{\mathrm{B}} T} \tag{4}$$

where N_{A} denotes Avogadro's constant and Z_i is the valence of the ion. We fixed the dielectric value interior the membrane (ε_m) as 2[40,41] and the permittivity of the solvent (ε_s) as 78.5. $k_{\mathrm{B}}T$ and d are employed as the units for energy and distance, respectively.

We employ the harmonic angular potential (U_{Angle}) to tailor the intrinsic rigidity of the polyelectrolyte chain,

$$U_{\mathrm{Angle}} = \sum_{i=2}^{N} k_{\mathrm{ang}}(\alpha_i - \alpha_0)^2 \tag{5}$$

where α_i is the angle of connected beads and $\alpha_0 = 180°$. We utilize the parameter k_{ang} ($[k_{\mathrm{B}}T/\mathrm{deg}^2]$) to adjust this angular potential and thus the chain intrisic rigidity.

Our implicit solvent model based on Debye−Hückel approximation cannot account for the effects of ionic fluctuations and correlations in the solvent caused by the electrostatic interaction,[42−44] which may affect the dependence of chain rigidity on the ionic concentration due to the electrostatic contribution.[45] Our present work instead mainly focuses on the effects of polyelectrolyte intrinsic rigidity on the complex structure, and therefore, we think that this coarse-grained model, along with further improvement thereof, could serve as one of the most effective computational strategies to elucidate some fundamental physical effects in the polyelectrolyte/monolayer interaction.[24,35,38,40,46,47]

2.2. Simulation Details. We employ the method proposed by Kawasaki[31,48,49] to model the movements of anionic lipids, and adopt the kink-jump, pivot, crankshaft and translation movements to model the polyelectrolyte relaxations. The simulation is performed by means of periodic boundary conditions in the x and y directions, and the position updates

DOI: 10.1021/acs.jpcb.5b00515
J. Phys. Chem. B 2015, 119, 6041−6049

Table 1. Total Persistence Length L_p (Å) of the Polyelectrolyte as a Function of the Rigidity Parameter k_{ang} at Different Bead Charge Densities Z_b of the Polyelectrolyte and Salt Solution Ionic Strength C_i

	L_p[Å]					
	k_{ang} [k_BT/deg^2] = 0	k_{ang} [k_BT/deg^2] = 0.003	k_{ang} [k_BT/deg^2] = 0.006	k_{ang} [k_BT/deg^2] = 0.015	k_{ang} [k_BT/deg^2] = 0.03	k_{ang} [k_BT/deg^2] = 0.06
			Z_b = +1			
C_i = 1 M/κ^- = 3 Å	27.3	34.0	39.7	46.7	49.1	55.1
C_i = 0.1 M/κ^- = 10 Å	31.8	37.0	42.0	49.4	53.8	58.7
C_i = 0.06 M/κ^- = 13 Å	34.6	40.0	45.0	52.8	56.8	59.9
C_i = 0.03 M/κ^- = 18 Å	39.4	44.0	48.5	55.3	59.1	65.1
C_i = 0.01 M/κ^- = 30 Å	47.4	49.5	51.2	56.8	60.7	66.7
C_i = 0.001 M/κ^- = 96 Å	57.1	58.5	60.1	62.6	67.7	71.0
			Z_b = +2			
C_i = 1 M/κ^- = 3 Å	27.2	34.2	39.8	46.6	49.3	55.0
C_i = 0.1 M/κ^- = 10 Å	38.1	41.8	45.2	50.0	57.0	59.7
C_i = 0.06 M/κ^- = 13 Å	46.7	48.1	50.4	56.0	63.2	72.2
C_i = 0.03 M/κ^- = 18 Å	58.3	59.7	62.0	66.3	70.4	78.1
C_i = 0.01 M/κ^- = 30 Å	75.3	79.3	80.6	82.1	91.2	92.3
C_i = 0.001 M/κ^- = 96 Å	86.6	91.5	95.9	102.3	107.9	110.1

Table 2. Typical Equilibrated Conformations of the Polyelectrolyte/Monolayer Complexes as a Function of the Chain Rigidity Parameter (k_{ang}), the Bead Charge Density (Z_b) of the Polyelectrolyte and the Salt Solution Ionic Strength (C_i)

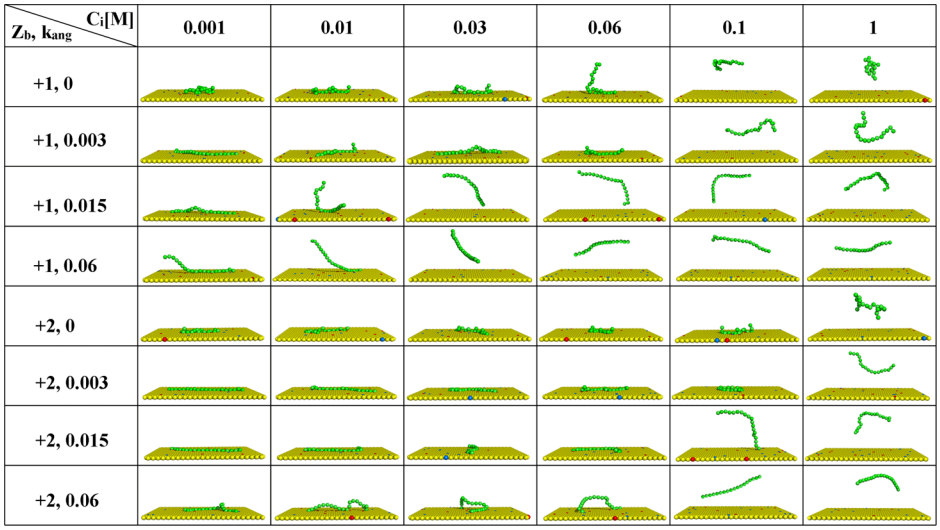

of the polyelectrolyte beads and the lipids satisfy the Metropolis algorithm,[50] with the acceptance rates higher than 20%. We vary the chain rigity parameter (k_{ang}) from 0 to 0.06 [k_BT/deg^2], and the charge density of each polyelectrolyte bead (Z_b) from +1 to +2. We also change the ionic concentration and the corresponding Debye screening length from C_i = 0.001 M (κ^{-1} = 96 Å) to C_i = 1 M (κ^{-1} = 3 Å).

At the very beginning of the simulation, we place the polyelectrolyte chain onto the lipid monolayer and randomly generate all anionic lipids on the monolayer. We first perform 1 × 10^6 MC steps of athermal relaxation to eliminate the potential artificial effects arising from the configuration initialization. Then, we employ 2 × 10^6 MC steps to achieve the system equilibration, within which the polyelectrolyte interacts with the membrane via U_{H-S}, U_{Coul}, and U_{Angle}. Finally, we evaluate the system properties from the ensemble average in another 2 × 10^6 MC steps. For each system, we obtain the final statistically averaged results from 20 parallel simulations.

2.3. Equilibrium Properties. We utilize the radial distribution functions (RDF) to examine redistribution of different anionic lipids, and calculate the orthogonal ($\langle R_g^2\rangle_O$) and parallel ($\langle R_g^2\rangle_P$) components of the mean-square radius of gyration $\langle R_g^2\rangle$ and bead number in tails, loops and trains of the chain to characterize the corresponding structural variation of the polyelectrolyte.[35] We calculate the monolayer surface coverage ratio $\theta = a_bN^*/a_m$, where N^* represents the bead number in train of the adsorbing polyelectrolyte, a_b and a_m denote the projected area of a bead and the total area of the membrane, respectively. We also analyze the polyelectrolyte adsorption amount $\Gamma = \theta/\theta_m$, where $\theta_m = Na_0/a_s$ denotes the maximum coverage ratio of the chain on monolayer.

We further calculate the polyelectrolyte chain persistence length L_p (Å), which includes the intrinsic rigidity of the polyelectrolyte L_0 and the electrostatic contribution L_e, according to the bond angle correlation function BAC[46]

$$\mathrm{BAC}(k) \sim \exp\left(-\frac{k}{L_p}\right) \tag{6}$$

where k represents the contour distance along the chain. In Table 1, we show the monotonic increase of total polyelectrolyte persistence length L_p with increasing the chain

DOI: 10.1021/acs.jpcb.5b00515
J. Phys. Chem. B 2015, 119, 6041−6049

intrinsic rigidity and the bead charge density, or decreasing the ionic strength.

3. RESULTS AND DISCUSSION

Of particular interest in our work is the interfacial structure variations of the polyelectrolyte/monolayer complexes. In Table 2, we first display a complete schematic view of the system by presenting the typical equilibrated conformations of the polyelectrolyte/monolayer complexes as a function of the chain rigidity parameter (k_{ang}), the bead charge density (Z_b) of the polyelectrolyte and the ionic strength of the salt solution (C_i), where the monolayer compositions is PC:PS:PIP_2 = 98:1:1.

3.1. Adsorption/Desorption Transition. We adjust the ionic concentration of the salt solution (C_i) to investigate the adsorption/desorption transition of the polyelectrolyte on lipid monolayer. We consider the polyelectrolyte "adsorb" on the monolayer if the chain keeps contacting with the monolayer surface for more than 50% of all MC steps in ensemble average, and define the C_i at such adsorption/desorption transition as the critical ionic concentration C_i^C. Correspondingly, the κ^- at C_i^C is named as the critical Debye screening length, denoted as κ_C^-. Figure 1 displays C_i^C as a function of the chain rigidity

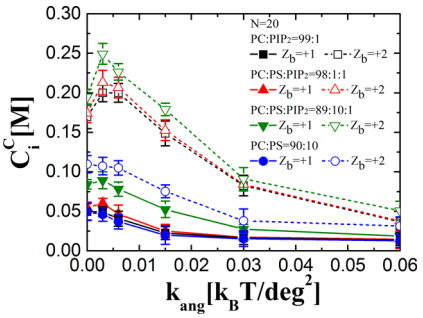

Figure 1. Critical ionic concentration (C_i^C) for adsorption/desorption transition of the polyelectrolyte/monolayer complex as a function of the chain rigidity parameter (k_{ang}) for different bead charge densities (Z_b) of the polyelectrolyte and monolayer compositions.

parameter (k_{ang}) for different bead charge densities (Z_b = +1 and Z_b = +2) of the polyelectrolyte and monolayer compositions (PC:PIP_2 = 99:1, PC:PS:PIP_2 = 98:1:1, PC:PS:PIP_2 = 89:10:1, and PC:PS = 90:10).

For polyelectrolyte with charge density Z_b = +1 (solid symbols and lines in Figure 1), C_i^C of polyelectrolyte/monolayer complex is relatively low. In the system with PC:PIP_2 = 99:1, C_i^C exhibits a plateau at 0.049 M when the rigidity parameter k_{ang} of the polyelectrolyte is less than 0.06 [k_BT/deg^2]. As k_{ang} increases, C_i^C decreases gradually from 0.049 M to a plateau value of 0.01 M, meaning that an increase in the degree of chain rigidity rapidly promotes the polyelectrolyte dissociation from the lipid monolayer. Because of the restricted rotations, the polyelectrolyte chain with increased intrinsic rigidity exhibits less entropy loss compared to the flexible ones while flattening onto the monolayer. This decreased entropy loss promotes the polyelectrolyte adsorption, whereas a larger demixing entropy loss is required for the PIP_2 lipid segregation underneath the stiffer polyelectrolyte, which promotes the polyelectrolyte/monolayer dissociation. On the other hand, the complex could be considered as an assemble of the dipoles composed of the cationic beads and the anionic lipids. The increase of the chain intrinsic rigidity inhibits the dipole−dipole aggregation, resulting in the decreased electrostatic energy gain, which also promotes the polyelectrolyte/monolayer dissociation. All these entropic and energetic factors compete to determine the finial structure of the complex. In the system with PC:PS:PIP_2 = 98:1:1, the additional 1% monovalent PS anionic lipids contribute to a decrease in the segregated multivalent PIP_2 lipid demixing entropy loss, and therefore, compared with the case of PC:PIP_2 = 99:1, with k_{ang} increasing from 0 to 0.003 [k_BT/deg^2], C_i^C increases. When k_{ang} > 0.003 [k_BT/deg^2], the increase of the lipid demixing entropy loss dominates the energy-entropy competition, and therefore, C_i^C decreases with k_{ang} from 0.06 M to a plateau value of 0.01 M. In the system with PC:PS:PIP_2 = 89:10:1, the 10% PS lipids drastically reduces the anionic lipid demixing entropy loss, therefore, C_i^C shows the similar tendency but much higher value than that for PC:PS:PIP_2 = 98:1:1. In the case of PC:PS = 90:10, C_i^C displays a monotonic decrease with the increase in k_{ang} and reaches a constant value for sufficiently large k_{ang}. For polyelectrolyte with charge density Z_b = +2 (vacant symbols and dashed lines in Figure 1), the polyelectrolyte/monolayer adsorption enhances significantly, and therefore, C_i^C increases drastically. For the polyelectrolyte adsorbing on monolayer containing PIP_2, we observe similar qualitative dependence of C_i^C on k_{ang}, i.e., C_i^C increases for semiflexible chains, and the adsorption/desorption transition takes place at a lower C_i^C as the chain rigidity further increases. In comparison, C_i^C in the system with PC:PS = 90:10 is low and decreases monotonically with k_{ang}.

In summary, the polyelectrolyte/monolayer association is achieved when electrostatic energy gains conquer over the entropic penalties caused by the loss of polyelectrolyte flexibility and lipid mixing freedom. A larger k_{ang} leads to the less polyelectrolyte conformational entropy loss, the larger segregated lipid demixing entropy loss, and the less electrostatic energy gains from charge neutralization, which compete to determine C_i^C at the adsorption/desorption transition. Previous Monte Carlo simulations have shown that on a uniformly charged surface[46] or a net-neutral lipid membrane containing both cationic and anionic lipids, because of the energy−entropy balance, the adsorption is stronger for a flexible polyelectrolyte as compared to a stiffer one.[30] Our results illustrate that, the adsorption strength between cationic polyelectrolyte and lipid monolayer of PC:PS = 90:10 exhibits a similar dependence on the chain rigidity, whereas on the monolayer containing multivalent lipids, compared with the flexible and rigid ones, the semiflexible polyelectrolyte chain can achieve the adsorption below a higher critical ionic concentration.

3.2. Rearrangement of the Anionic Lipids. Differing from the charged macromolecule adsorption on uniformly charged surface or membrane with fixed charged lipids,[24,30,51−53] the mobile anionic lipids can migrate in the monolayer to influence the behavior of the polyelectrolyte. In Figure 2, we present the radial distribution functions (RDF) of the anionic lipids to illustrate the lipid rearrangement in monolayer with PC:PS:PIP_2 = 98:1:1 induced by polyelectrolyte attraction. The RDF of PIP_2−PIP_2 lipids and PS−PS lipids are denoted as $g_{PIP2}(r)$ and $g_{PS}(r)$, respectively.

In Figure 2, parts a and h, we first present the $g_{PIP2}(r)$ and $g_{PS}(r)$ for the bare monolayer at different ionic concentrations C_i, respectively. Before the polyelectrolyte adsorption, the electrostatic repulsions prevent the PIP_2 lipids or PS lipids from approaching each other, and thus, both $g_{PIP2}(r)$ and $g_{PS}(r)$ increase with r and gradually reach a constant of 1 at large r

DOI: 10.1021/acs.jpcb.5b00515
J. Phys. Chem. B 2015, 119, 6041−6049

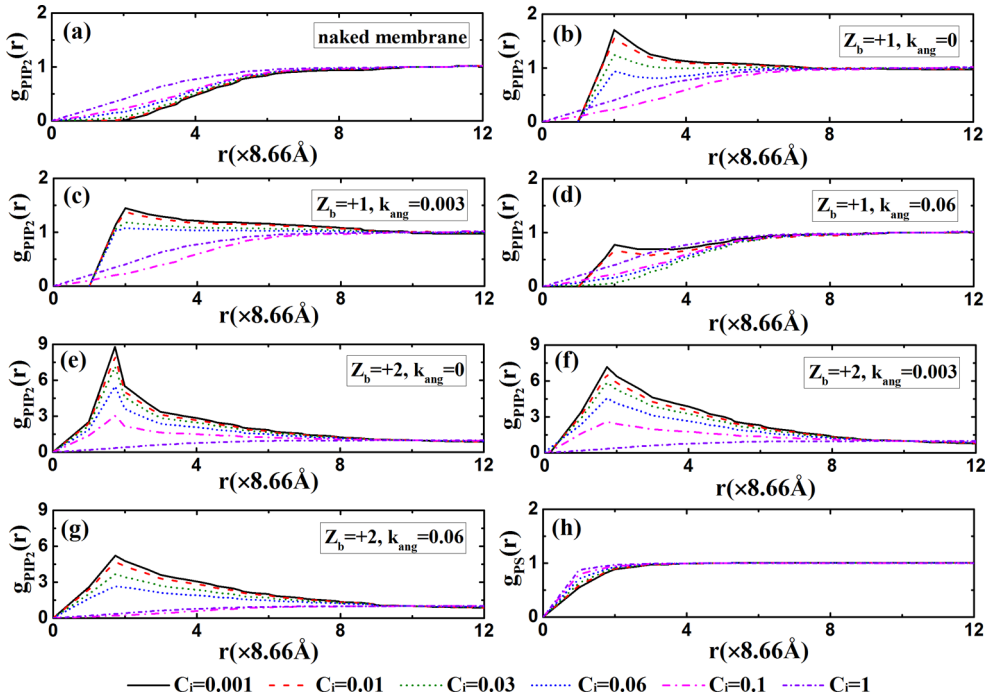

Figure 2. Radial distribution functions for PIP_2 lipids and PS lipids as a function of the chain rigidity parameter (k_{ang}) for different bead charge density (Z_b) of the polyelectrolyte and solution ionic strength (C_i). PC:PS:PIP_2 = 98:1:1.

under different C_i. In Figure 2b, we show the effects of the adsorbing flexible polyelectrolyte (k_{ang} = 0, Z_b = +1) on $g_{PIP2}(r)$. When C_i = 0.001 M, $g_{PIP2}(r)$ exhibits a peak value at r = 2 (×8.66 Å), which is caused by the electrostatic attraction from the polyelectrolyte. With C_i increasing to C_i^C=0.06 M, the stronger electrostatic screening effect from the solution results in the polyelectrolyte/monolayer dissociation, and therefore, the peaks at r = 2 (×8.66 Å) exhibits a significant decrease. The lateral segregation of charged lipids is weakened by the increase of ionic concentration, which is in agreement with previous experiments.[8] By increasing the chain rigidity parameter k_{ang} to 0.003 [k_BT/deg^2] (Figure 2c), when $C_i < C_i^C$, the $g_{PIP2}(r)$ values decrease at r < 3 (×8.66 Å) and increase slightly at r > 3 (×8.66 Å), indicating that compared with the flexible one, the adsorbing semiflexible chain with more stretched conformation can segregate the PIP_2 lipids in a least compact way. On the other hand, in Figure 2d, with the further increase of chain rigidity parameter to k_{ang} > 0.015 [k_BT/deg^2], the rigid rod-like polyelectrolyte starts to dissociate from the lipid monolayer, and thus fewer PIP_2 lipids are segregated, resulting in the significant decrease of $g_{PIP2}(r)$ at r < 10 (× 8.66 Å). Furthermore, in Figure 2e–g, for the polyelectrolyte with charge density of +2, because of the larger charge taken by the bead, the electrostatic energy gain in the polyelectrolyte/monolayer association dominates over the energy–entropy competition, therefore the polyelectrolyte with any intrinsic rigidity parameter can segregate a larger amount of PIP_2 lipids compactly. The peak value of $g_{PIP2}(r)$ at small r exhibits a dramatic increase for the adsorption of polyelectrolyte with different k_{ang} in comparison with the case of Z_b = +1. In addition, we find that in the monolayer, even if the PIP_2 lipids significantly enrich underneath the polyelectrolyte, the corresponding $g_{PS}(r)$ values are still the same as that for naked membrane (Figure 2h), illustrating the dominant role of PIP_2 in polyelectrolyte association. Although the PS lipids contribute to a reduction in the PIP_2 demixing entropy loss, the distribution of PS lipids is independent of the effects of polyelectrolyte chain rigidity.

We also investigate the RDF variation of different anionic lipids induced by polyelectrolyte attraction when the monolayer compositions are PC:PIP_2 = 99:1, PC:PS:PIP_2 = 89:10:1, and PC:PS:PIP_2 = 90:10. The readers are referred to the results of RDF for these systems in Figures S1, S2, and S3 in the Supporting Information. In monolayer with PC:PS:PIP_2 = 89:10:1 and PC:PIP_2 = 99:1, the $g_{PIP2}(r)$ values display similar results as that in Figure 2. On the monolayer with PC:PS = 90:10 (Figure S3), the polyelectrolyte can also cause the PS clustering, whereas by increasing both k_{ang} and C_i, the polyelectrolyte tends to dissociate from the monolayer, therefore the $g_{PS}(r)$ displays a monotonic dependence on these two factors.

3.3. Structure of the Polyelectrolyte. To investigate the conformational variations of the polyelectrolyte chain in the association, in Figure 3 (PC:PS:PIP_2 = 98:1:1), we present the effects of chain rigidity parameter (k_{ang}) on the parallel ($\langle R_g^2\rangle_P$) and orthogonal ($\langle R_g^2\rangle_O$) components of $\langle R_g^2\rangle$ of the polyelectrolyte. For the flexible polyelectrolyte with Z_b = +1 (Figure 3, parts a and b), with the increase of the Debye screening length κ^- from 3 to 96 Å, the polyelectrolyte experiences the desorption-adsorption transition, with its structure changing from a random-coil-like conformation in the solution to a pancake-like conformation on the monolayer (see Table 2). The corresponding $\langle R_g^2\rangle_O$ displays a dramatic decrease and $\langle R_g^2\rangle_P$ exhibits a noticeable increase. Our results are qualitatively consistent with the results of the previous Monte Carlo simulation[51] and molecular dynamics simulation,[52] where the conformation of the adsorbing polyelectrolyte was investigated on the oppositely charged surface with a uniform charge density. The mobile anionic lipids segregate around the polyelectrolyte to neutralize the electrostatic repulsion between the cations on the polyelectrolyte, and therefore, our results show that both $\langle R_g^2\rangle_P$ and $\langle R_g^2\rangle_O$ of the

DOI: 10.1021/acs.jpcb.5b00515
J. Phys. Chem. B 2015, 119, 6041–6049

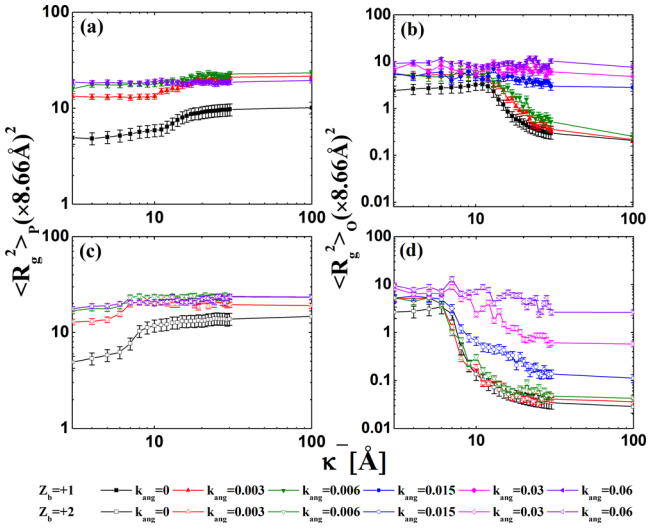

Figure 3. Parallel ($\langle R_g^2\rangle_P$) and orthogonal ($\langle R_g^2\rangle_O$) components of the mean-square radius of gyration of the polyelectrolyte as a function of the rigidity parameter (k_{ang}) for different bead charge density (Z_b) of the polyelectrolyte and Debye screening length of the solution (κ^-). PC:PS:PIP$_2$ = 98:1:1.

adsorbing polyelectrolyte exhibit smaller values than the cases of adsorption on uniform charged surface. This finding suggests that the membrane fluidity could be essential for the conformation variations of the adsorbing polyelectrolyte. In addition, our work further indicates that, the adsorbing semiflexible polyelectrolyte (k_{ang} = 0.03, 0.06 [k_BT/deg^2]) displays a more stretched conformation, with a dramatic increase of $\langle R_g^2\rangle_P$. Whereas for the rigid polyelectrolyte (k_{ang} >0.015 [k_BT/deg^2]), the chain cannot bind firmly and starts to dissociate from the monolayer, therefore, the corresponding $\langle R_g^2\rangle_P$ and $\langle R_g^2\rangle_O$ cannot vary as significantly as that of the flexible and semiflexible chains during the desorption-adsorption transition (κ^- from 3 to 96 Å). For the polyelectrolyte with charge density of +2 (In Figure 3c and 3d), when $\kappa^- > \kappa_C^-$, the adsorption ability of the polyelectrolyte with different rigidity enhances significantly, and the adsorbing polyelectrolyte shows more flatten conformation with smaller $\langle R_g^2\rangle_O$ than the one with Z$_b$=+1.

In Figure 4, we further discuss the structure of the adsorbing polyelectrolyte on the monolayer with PC:PS:PIP$_2$ = 98:1:1 by showing the number of beads in trains, loops, and tails of the polyelectrolyte as a function of k_{ang}, Z_b, and C_i. For the polyelectrolyte with Z_b = +1, as shown in Figure 4a, most beads present in trains in the case of flexible polyelectrolyte adsorption when C_i is less than 0.01 M. Because of the effects of the mobile anionic lipids, the polyelectrolyte presents smaller tails or loops and exhibits more flattened conformation on the charged membrane than the one adsorbing on the uniformly charged surface predicted by previous Monte Carlo[53] and molecular dynamics[52] simulations. In fact, our results also support the conclusion that the mobile charged lipids embedded in the membrane surface adsorb a higher number of monomers from both flexible and semiflexible polyelectrolytes than the fixed ones on the surface.[24,30] By increasing C_i to C_i^C, the stronger screening effects from the saline solution significantly weakens the association of the polyelectrolyte, and therefore, both bead numbers of loops and tails enlarge to a maximal value at the sacrifice in the size of the trains. Then, the polyelectrolyte desorbs when C_i is higher than C_i^C, resulting in a rapid decrease in the sizes of trains, loops, and tails. For the

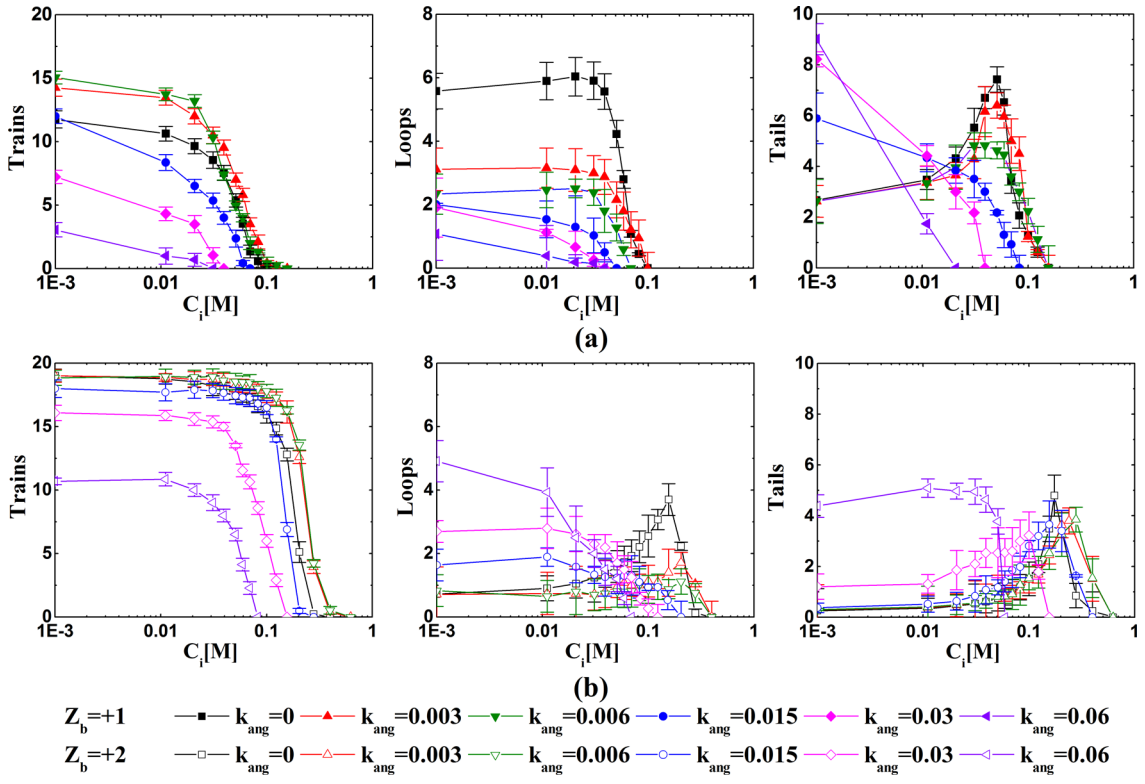

Figure 4. Number of beads in trains, loops, and tails of the polyelectrolyte as a function of the rigidity parameter (k_{ang}) for different charge density (Z_b) of the polyelectrolyte and salt solution ionic strength (C_i). PC:PS:PIP$_2$ = 98:1:1.

DOI: 10.1021/acs.jpcb.5b00515
J. Phys. Chem. B 2015, 119, 6041−6049

semiflexible chain (k_{ang} = 0.003, 0.006 [k_BT/deg^2]), when C_i < C_i^C, compared with the flexible one, the trains enlarge, whereas the loops and tails shrink, because the polyelectrolyte loses less entropy while adsorbing onto the monolayer. With the further increase of chain rigidity parameter to k_{ang} > 0.015 [k_BT/deg^2], compared with cases for the flexible and semiflexible chains at C_i < 0.01 M, the sizes of both trains and loops reduce dramatically, whereas the tails enlarge significantly. With C_i increasing, the rigid chain dissociates quickly. For the polyelectrolyte with Z_b = +2 (Figure 4b), when C_i < C_i^C, stronger electrostatic attractions strengthen the polyelectrolyte/monolayer adsorption, resulting in the significant enlargement of trains as compared with the chain with Z_b = +1. The semiflexble polyelectrolyte chain (k_{ang} = 0.03, 0.06 [k_BT/deg^2]) flattens on the monolayer with much smaller sizes of the loops and tails. When k_{ang} > 0.015 [k_BT/deg^2], to avoid the highly demixing distribution underneath the very rigid polyelectrolyte, only few anionic lipids migrate to associate with it. Whereas, the stronger electrostatic interactions between the mobile PIP_2 and the polyelectrolyte beads with Z_b = +2 prevent the chain from presenting large tails but force it to form a bridge-like conformation on the monolayer with larger loops, a result that is quite different from Figure 4a.

In the Supporting Information, we also show the effects of chain rigidity on the structural variations of the polyelectrolyte adsorbing on lipid monolayer with different compositions (Figure S4 and S5). On the ternary monolyer (PC:PS:PIP_2 = 89:10:1), the chain can bind on the membrane surface more firmly. However, on the binary monolayer with neutral and monovalent lipids (PC:PS = 90:10), in the absence of PIP_2, the polyelectrolyte/monolayer association is relatively weakened.

3.4. Adsorption Amount and Surface Coverage Ratio.

In Figure 5, we display the dependence of the polyelectrolyte adsorption amount (Γ) and the monolayer surface coverage ratio (θ) on the chain rigidity parameter (k_{ang}), the bead charge density (Z_b) of the polyelectrolyte and the salt solution ionic strength (C_i), when the monolayer composition is PC:PS:PIP_2 = 98:1:1. Both Γ and θ decrease with the increase of C_i because of the polyelectrolyte dissociation. For semiflexible polyelectrolyte with Z_b=+1 (Figure 5a), when C_i < C_i^C, Γ and θ are larger than that for the flexible one. In these cases, Γ and θ exhibit a maximum corresponding to the formation of a flatten stretched conformation with few parts extending in the solution. When k_{ang} > 0.015 [k_BT/deg^2], Γ and θ decrease dramatically in the regime C_i<C_i^C, with the exact value dependent on k_{ang} and C_i. For polyelectrolyte with charge density of +2 (Figure 5b), due to stronger electrostatic attractions between beads and anionic lipids, the chain associate onto the monolayer more firmly, resulting in a significant increase of Γ and θ. In summary, we demonstrate that both the polyelectrolyte adsorption amount (Γ) and the monolayer surface coverage ratio (θ) exhibit nonmonotonic dependences on the chain rigidity k_{ang}, but monotonic dependences on the bead charge density Z_b and the saline solution ionic strength C_i.

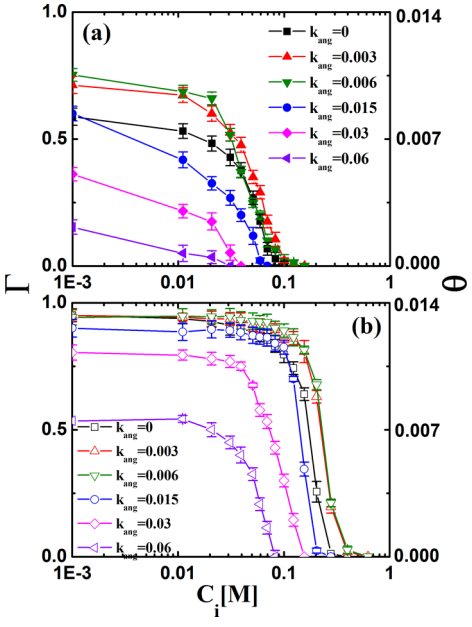

Figure 5. Polyelectrolyte adsorption amount (Γ) and monolayer surface coverage ratio (θ) as a function of the chain rigidity parameter (k_{ang}) for different bead charge density (Z_b) of the polyelectrolyte and salt solution ionic strength (C_i). PC:PS:PIP_2 = 98:1:1.

4. CONCLUSION

We constructe a Monte Carlo model to investigate the adsorption of a positively charged polyelectrolyte on a lipid monolayer, composed of neutral, monovalent, and multivalent anionic phospholipids, and systematically explore the effects of chain intrinsic rigidity on the interfacial structural properties of the polyelectrolyte/monolayer complex at different bead charge density of the polyelectrolyte and saline solution ionic strength. The enhancement of the chain intrinsic rigidity reduces the polyelectrolyte conformational entropy loss and the electrostatic energy gains but elevates the anionic lipid demixing entropy loss. This energy−entropy competition results in a nonmonotonic dependence of the polyelectrolyte/monolayer association strength on the chain intrinsic rigidity. Compared with the flexible and rigid ones, the semiflexible polyelectrolyte exhibits stronger association onto the ternary monolayer, below a higher critical ionic concentration. In this ionic concentration regime, the adsorbing flexible polyelectrolyte chain displays a pancake-like conformation on the monolayer, whereas the semiflexible one adsorbs onto the membrane in a more flattened and stretched structure, with the multivalent anionic lipids incompactly segregated underneath it. For the rigid chain, the energy-entropy competition results in the formation of large tails for the polyelectrolyte with charge density of Z_b = +1 and a bridge-like conformation for the one with Z_b = +2 on the monolayer. Our findings provide novel insight for elucidating the mechanism of the polyelectrolyte/monolayer interaction and are helpful for the selection of proteins and polypeptides in the controlled release of the signaling lipids.

■ ASSOCIATED CONTENT

Supporting Information

Rearrangement of PIP_2 and PS lipids and the structural variation of the polyelectrolyte in the system with different monolayer compositions. The Supporting Information is available free of charge on the ACS Publications website at DOI: 10.1021/acs.jpcb.5b00515.

■ AUTHOR INFORMATION

Corresponding Authors

*(T.S.) E-mail: tfshi@ciac.ac.cn. Telephone: 86-431-85262309.
*(W.-S.X.) E-mail: wsxu@uchicago.edu. Telephone: 1-773-366-0112.

DOI: 10.1021/acs.jpcb.5b00515
J. Phys. Chem. B 2015, 119, 6041−6049

Notes

The authors declare no competing financial interest.

■ ACKNOWLEDGMENTS

This work was supported by the National Natural Science Foundation of China (51028301, 51473168, 21234007, 21174146, 21404103). We are grateful to the Computing Center of Jilin Province for essential support.

■ REFERENCES

(1) McLaughlin, S.; Murray, D. Plasma Membrane Phosphoinositide Organization by Protein Electrostatics. *Nature* **2005**, *438*, 605−611.
(2) Czech, M. P. PIP_2 and PIP_3: Complex Roles at the Cell Surface. *Cell* **2000**, *100*, 603−606.
(3) Vance, J. E.; Steenbergen, R. Metabolism and Functions of Phosphatidylserine. *Prog. Lipid Res.* **2005**, *44*, 207−234.
(4) Di Paolo, G.; De Camilli, P. Phosphoinositides in Cell Regulation and Membrane Dynamics. *Nature* **2006**, *443*, 651−657.
(5) Lemmon, M. A. Phosphoinositide Recognition Domains. *Traffic* **2003**, *4*, 201−213.
(6) Yeung, T.; Gilbert, G. E.; Shi, J.; Silvius, J.; Kapus, A.; Grinstein, S. Membrane Phosphatidylserine Regulates Surface Charge and Protein Localization. *Science* **2008**, *319*, 210−213.
(7) Wang, J. Y.; Gambhir, A.; Hangyas-Mihalyne, G.; Murray, D.; Golebiewska, U.; McLaughlin, S. Lateral Sequestration of Phosphatidylinositol 4,5-bisphosphate by the Basic Effector Domain of Myristoylated alanine-rich C Kinase Substrate is due to Nonspecific Electrostatic Interactions. *J. Biol. Chem.* **2002**, *277*, 34401−34412.
(8) Gambhir, A.; Hangyas-Mihalyne, G.; Zaitseva, I.; Cafiso, D. S.; Wang, J. Y.; Murray, D.; Pentyala, S. N.; Smith, S. O.; McLaughlin, S. Electrostatic Sequestration of PIP_2 on Phospholipid Membranes by Basic/aromatic Regions of Proteins. *Biophys. J.* **2004**, *86*, 2188−2207.
(9) Kim, J. Y.; Mosior, M.; Chung, L. A.; Wu, H.; McLaughlin, S. Binding of Peptides with Basic Residues to Membranes Containing Acidic Phospholipids. *Biophys. J.* **1991**, *60*, 135−148.
(10) Cai, X. M.; Lietha, D.; Ceccarelli, D. F.; Karginov, A. V.; Rajfur, Z.; Jacobson, K.; Hahn, K. M.; Eck, M. J.; Schaller, M. D. Spatial and Temporal Regulation of Focal Adhesion Kinase Activity in Living Cells. *Mol. Cell. Biol.* **2008**, *28*, 201−214.
(11) Sarkar, J.; Annepu, H.; Sharma, A. Contact Instability of a Soft Elastic Film Bonded to a Patterned Substrate. *J. Adhes.* **2011**, *87*, 214−234.
(12) Ferguson, C. G.; James, R. D.; Bigman, C. S.; Shepard, D. A.; Abdiche, Y.; Katsamba, P. S.; Myszka, D. G.; Prestwich, G. D. Phosphoinositide-containing Polymerized Liposomes: Stable Membrane-mimetic Vesicles for Protein-lipid Binding Analysis. *Bioconjugate Chem.* **2005**, *16*, 1475−1483.
(13) Yan, H. D.; Villalobos, C.; Andrade, R. TRPC Channels Mediate a Muscarinic Receptor-Induced Afterdepolarization in Cerebral Cortex. *J. Neurosci.* **2009**, *29*, 10038−10046.
(14) Yeh, L. H.; Xue, S.; Joo, S. W.; Qian, S.; Hsu, J. P. Field Effect Control of Surface Charge Property and Electroosmotic Flow in Nanofluidics. *J. Phys. Chem. C* **2012**, *116*, 4209−4216.
(15) Mollapour, M.; Phelan, J. P.; Millson, S. H.; Piper, P. W.; Cooke, F. T. Weak Acid and Alkali Stress Regulate Phosphatidylinositol Bisphosphate Synthesis in Saccharomyces Cerevisiae. *Biochem. J.* **2006**, *395*, 73−80.
(16) Im, Y. J.; Perera, I. Y.; Brglez, I.; Davis, A. J.; Stevenson-Paulik, J.; Phillippy, B. Q.; Johannes, E.; Allen, N. S.; Boss, W. F. Increasing Plasma Membrane Phosphatidylinositol(4,5)bisphosphate Biosynthesis Increases Phosphoinositide Metabolism in Nicotiana Tabacum. *Plant Cell* **2007**, *19*, 1603−1616.
(17) Mitrakos, P.; Macdonald, P. M. Polyelectrolyte molecular weight and electrostatically-induced domains in lipid bilayer membranes. *Biomacromolecules* **2000**, *1*, 365−376.
(18) Murray, D.; Arbuzova, A.; Honig, B.; McLaughlin, S. The Role of Electrostatic and Nonpolar Interactions in the Association of Peripheral Proteins with Membranes. *Curr. Top. Membr.* **2002**, *52*, 277−307.
(19) Golebiewska, U.; Nyako, M.; Woturski, W.; Zaitseva, I.; McLaughlin, S. Diffusion Coefficient of Fluorescent Phosphatidylinositol 4,5-bisphosphate in the Plasma Membrane of Cells. *Mol. Biol. Cell* **2008**, *19*, 1663−1669.
(20) Dietrich, U.; Kruger, P.; Gutberlet, T.; Kas, J. A. Interaction of the MARCKS Peptide with PIP_2 in Phospholipid Monolayers. *BBA-Biomembranes* **2009**, *1788*, 1474−1481.
(21) Deme, B.; Hess, D.; Tristl, M.; Lee, L. T.; Sackmann, E. Binding of Actin Filaments to Charged Lipid Monolayers: Film Balance Experiments Combined with Neutron Reflectivity. *Eur. Phys. J. E* **2000**, *2*, 125−136.
(22) Honda, A.; Nogami, M.; Yokozeki, T.; Yamazaki, M.; Nakamura, H.; Watanabe, H.; Kawamoto, K.; Nakayama, K.; Morris, A. J.; Frohman, M. A.; Kanaho, Y. Phosphatidylinositol 4-phosphate 5-kinase Alpha Is a Downstream Effector of the Small G Protein ARF6 in Membrane Ruffle Formation. *Cell* **1999**, *99*, 521−532.
(23) Tall, E. G.; Spector, I.; Pentyala, S. N.; Bitter, I.; Rebecchi, M. J. Dynamics of Phosphatidylinositol 4,5-Bisphosphate in Actin-rich Structures. *Curr. Biol.* **2000**, *10*, 743−746.
(24) Tzlil, S.; Ben-Shaul, A. Flexible Charged Macromolecules on Mixed Fluid Lipid Membranes: Theory and Monte Carlo Simulations. *Biophys. J.* **2005**, *89*, 2972−2987.
(25) Heo, W. D.; Inoue, T.; Park, W. S.; Kim, M. L.; Park, B. O.; Wandless, T. J.; Meyer, T. $PI(3,4,5)P_3$ and $PI(4,5)P_2$ Lipids Target Proteins with Polybasic Clusters to the Plasma Membrane. *Science* **2006**, *314*, 1458−1461.
(26) Golebiewska, U.; Gambhir, A.; Hangyas-Mihalyne, G.; Zaitseva, I.; Radler, J.; McLaughlin, S. Membrane-bound Basic Peptides Sequester Multivalent (PIP_2), but not Monovalent (PS), Acidic Lipids. *Biophys. J.* **2006**, *91*, 588−599.
(27) Haleva, E.; Ben-Tal, N.; Diamant, H. Increased Concentration of Polyvalent Phospholipids in the Adsorption Domain of a Charged Protein. *Biophys. J.* **2004**, *86*, 2165−2178.
(28) Mbamala, E. C.; Ben-Shaul, A.; May, S. Domain Formation Induced by the Adsorption of Charged Proteins on Mixed Lipid Membranes. *Biophys. J.* **2005**, *88*, 1702−1714.
(29) Loew, S.; Hinderliter, A.; May, S. Stability of Protein-decorated Mixed Lipid Membranes: The Interplay of Lipid-lipid, Lipid-protein, and Protein-protein Interactions. *J. Chem. Phys.* **2009**, *130*, 045102.
(30) Dias, R. S.; Pais, A.; Linse, P.; Miguel, M. G.; Lindman, B. Polyion Adsorption onto Catanionic Surfaces. A Monte Carlo Study. *J. Phys. Chem. B* **2005**, *109*, 11781−11788.
(31) Kiselev, V. Y.; Marenduzzo, D.; Goryachev, A. B. Lateral Dynamics of Proteins with Polybasic Domain on Anionic Membranes: A Dynamic Monte-Carlo Study. *Biophys. J.* **2011**, *100*, 1261−1270.
(32) McLaughlin, S.; Wang, J. Y.; Gambhir, A.; Murray, D. PIP_2 AND Proteins: Interactions, Organization, and Information Flow. *Annu. Rev. Bioph. Biom.* **2002**, *31*, 151−175.
(33) Rusu, L.; Gambhir, A.; McLaughlin, S.; Radler, J. Fluorescence Correlation Spectroscopy Studies of Peptide and Protein Binding to Phospholipid Vesicles. *Biophys. J.* **2004**, *87*, 1044−1053.
(34) Tian, W. D.; Ma, Y. Q. Insights into the Endosomal Escape Mechanism via Investigation of Dendrimer-membrane Interactions. *Soft Matter* **2012**, *8*, 6378−6384.
(35) Duan, X. Z.; Zhang, R.; Li, Y. Q.; Shi, T. F.; An, L. J.; Huang, Q. R. Monte Carlo Study of Polyelectrolyte Adsorption on Mixed Lipid Membrane. *J. Phys. Chem. B* **2013**, *117*, 989−1002.
(36) Duan, X. Z.; Li, Y. Q.; Zhang, R.; Shi, T. F.; An, L. J.; Huang, Q. R. Regulation of Anionic Lipids in Binary Membrane upon the Adsorption of Polyelectrolyte: A Monte Carlo Simulation. *AIP Adv.* **2013**, *3*, 062128.
(37) Duan, X. Z.; Zhang, R.; Li, Y. Q.; Yang, Y. B.; Shi, T. F.; An, L. J.; Huang, Q. R. Effect of Polyelectrolyte Adsorption on Lateral Distribution and Dynamics of Anionic Lipids: A Monte Carlo Study of a Coarse-grain Model. *Eur. Biophys. J.* **2014**, *43*, 377−391.
(38) Duan, X. Z.; Li, Y. Q.; Zhang, R.; Shi, T. F.; An, L. J.; Huang, Q. R. Compositional Redistribution and Dynamic Heterogeneity in

DOI: 10.1021/acs.jpcb.5b00515
J. Phys. Chem. B 2015, 119, 6041−6049

Mixed Lipid Membrane Induced by Polyelectrolyte Adsorption: Effects of Chain Rigidity. *Eur. Phys. J. E* **2014**, *37*, 71.
(39) Wang, L.; Liang, H. J.; Wu, J. Z. Electrostatic Origins of Polyelectrolyte Adsorption: Theory and Monte Carlo Simulations. *J. Chem. Phys.* **2010**, *133*, 044906.
(40) Tzlil, S.; Murray, D.; Ben-Shaul, A. The "Electrostatic-Switch" Mechanism: Monte Carlo Study of MARCKS-membrane Interaction. *Biophys. J.* **2008**, *95*, 1745−1757.
(41) Khelashvili, G.; Weinstein, H.; Harries, D. Protein Diffusion on Charged Membranes: A Dynamic Mean-field Model Describes Time Evolution and Lipid Reorganization. *Biophys. J.* **2008**, *94*, 2580−2597.
(42) Reddy, G.; Yethiraj, A. Solvent Effects in Polyelectrolyte Adsorption: Computer Simulations with Explicit and Implicit Solvent. *J. Chem. Phys.* **2010**, *132*, 074903.
(43) Patra, C. N.; Yethiraj, A. Density Functional Theory for the Nonspecific Binding of Salt to Polyelectrolytes: Thermodynamic Properties. *Biophys. J.* **2000**, *78*, 699−706.
(44) Dobrynin, A. V.; Rubinstein, M. Theory of Polyelectrolytes in Solutions and at Surfaces. *Prog. Polym. Sci.* **2005**, *30*, 1049−1118.
(45) Murnen, H. K.; Rosales, A. M.; Dobrynin, A. V.; Zuckermann, R. N.; Segalman, R. A. Persistence Length of Polyelectrolytes with Precisely Located Charges. *Soft Matter* **2013**, *9*, 90−98.
(46) Stoll, S.; Chodanowski, P. Polyelectrolyte Adsorption on an Oppositely Charged Spherical Particle. Chain Rigidity Effects. *Macromolecules* **2002**, *35*, 9556−9562.
(47) Chodanowski, P.; Stoll, S. Polyelectrolyte Adsorption on Charged Particles in the Debye-Huckel Approximation. A Monte Carlo Approach. *Macromolecules* **2001**, *34*, 2320−2328.
(48) Kawasaki, K. In *Phase Transitions and Critical Phenomena*; Domb, C., Green, M. S., Eds.; Academic Press: New York, 1972; Vol. 2.
(49) Jan, N.; Lookman, T.; Pink, D. A. On Computer-Simulation Methods Used to Study Models of 2-Component Lipid Bilayers. *Biochemistry* **1984**, *23*, 3227−3231.
(50) Metropolis, N.; Rosenbluth, A. W.; Rosenbluth, M. N.; Teller, A. H.; Teller, E. Equation of State Calculations by Fast Computing Machines. *J. Chem. Phys.* **1953**, *21*, 1087−1092.
(51) Kong, C. Y.; Muthukumar, M. Monte Carlo Study of Adsorption of a Polyelectrolyte onto Charged Surfaces. *J. Chem. Phys.* **1998**, *109*, 1522−1527.
(52) Reddy, G.; Chang, R. W.; Yethiraj, A. Adsorption and Dynamics of a Single Polyelectrolyte Chain near a Planar Charged Surface: Molecular Dynamics Simulations with Explicit Solvent. *J. Chem. Theory Comput.* **2006**, *2*, 630−636.
(53) Narambuena, C. F.; Beltramo, D. M.; Leiva, E. P. M. Polyelectrolyte Adsorption on a Charged Surface. A Study by Monte Carlo Simulations. *Macromolecules* **2007**, *40*, 7336−7342.

DOI: 10.1021/acs.jpcb.5b00515
J. Phys. Chem. B 2015, 119, 6041−6049